

## Novel Superhard Carbon: C-Centered Orthorhombic C<sub>8</sub>

Zhisheng Zhao,<sup>1</sup> Bo Xu,<sup>1</sup> Xiang-Feng Zhou,<sup>2</sup> Li-Min Wang,<sup>1</sup> Bin Wen,<sup>1</sup> Julong He,<sup>1</sup>  
Zhongyuan Liu,<sup>1</sup> Hui-Tian Wang,<sup>2</sup> and Yongjun Tian<sup>1,\*</sup>

<sup>1</sup>State Key Laboratory of Metastable Materials Science and Technology, Yanshan University, Qinhuangdao 066004, China

<sup>2</sup>School of Physics and Key Laboratory of Weak-Light Nonlinear Photonics, Ministry of Education,  
Nankai University, Tianjin 300071, China

(Received 10 June 2011; published 14 November 2011)

A novel carbon allotrope of C-centered orthorhombic C<sub>8</sub> (Cco-C<sub>8</sub>) is predicted by using a recently developed particle-swarm optimization method on structural search. Cco-C<sub>8</sub> adopts a  $sp^3$  three-dimensional bonding network that can be viewed as interconnected (2, 2) carbon nanotubes through 4- and 6-member rings and is energetically more favorable than earlier proposed carbon polymorphs (e.g., *M* carbon, bct-C<sub>4</sub>, *W* carbon, and chiral C<sub>6</sub>) over a wide range of pressures studied (0–100 GPa). The simulated x-ray diffraction pattern, density, and bulk modulus of Cco-C<sub>8</sub> are in good accordance with the experimental data on structurally undetermined superhard carbon recovered from cold compression of carbon nanotube bundles. The simulated hardness of Cco-C<sub>8</sub> can reach a remarkably high value of 95.1 GPa, such that it is capable of cracking diamond.

DOI: 10.1103/PhysRevLett.107.215502

PACS numbers: 61.50.Ks, 61.48.De, 64.60.My

Carbon possesses the unique capability to form  $sp$ -,  $sp^2$ -, and  $sp^3$ -hybridized bonds, yielding various allotropes such as graphite, diamond, lonsdaleite, carbyne, chaoite, fullerenes, nanotubes, graphene, and so on. Pressure-induced changes of bonding from  $sp^2$  to  $sp^3$  for graphite, fullerenes, and carbon nanotubes (CNTs) have stimulated considerable scientific interest and are the key for producing new carbon phases with novel electronic properties and superior mechanical performances. A transparent superhard carbon phase was recently identified in a cold-compression experiment with graphite [1,2]. Distinct from diamond, this carbon polymorph is quenchable only at low temperatures (< 100 K) [1]. Several  $sp^3$ -hybridized structures (i.e., *M* carbon, bct-C<sub>4</sub>, and *W* carbon or their mixtures) have been proposed as the structural solution for this post-graphite phase [3–6]. Since the structures of recovered metastable phases depend strongly on the crystal structures and the hybridized forms of raw carbons, C<sub>60</sub> fullerenes under pressure were found to transform into interesting one-, two-, and three-dimensional (3D) polymers [7–10]. The compression of CNTs yields more exciting but intricate phases because of the complexity in diameters, lengths, and chirality of single- or multi-walled CNTs [11–15]. The challenge largely arises from the fact that new carbon products obtained from the compression of CNTs are often heterogeneous, consisting of several known phases (e.g., unreacted nanotubes, generative graphite, and amorphous carbon).

Hydrostatic or nonhydrostatic effects would also have direct influences on the produced carbon phases. Single-walled CNTs at room temperature are polygonized at a hydrostatic pressure of 1.5 GPa. The tube lattice is destroyed beyond 4 GPa [16]. At a pressure of 24 GPa, a new superhard carbon (hardness at 62–150 GPa) could be

synthesized under nonhydrostatic stress conditions [11,12]. Other new nano- and microcrystalline, diamond-like (cubic and hexagonal), and nanographite carbon phases have also been observed from treatments of single-walled CNTs under pressures of 8.0–9.5 GPa and at temperatures of 473–1773 K [13]. Under nonhydrostatic pressure conditions, multiwalled CNTs become partially transparent at 11 GPa and transform into a superhard phase with no contributions from  $sp^2$  bonds at 16 GPa [15]. Of particular interest is the recent observation of an unknown, but quenchable, superhard carbon allotrope recovered from direct compression at about 75 GPa of assembled nanotube bundles at room temperature [14]. The allotrope can crack diamonds; thus, great interest in the exploration of the crystal structure of this phase has been generated. A hexagonal structure composed of 3D interlinked share-wall (6, 0) nanotubes [3D-(6, 0) carbon] was subsequently proposed to interpret the experimental phase [17]. However, the simulated x-ray diffraction (XRD) pattern of 3D-(6, 0) carbon deviates largely from the experimental data. This motivates the search for a more precise structural model to understand this intriguing superhard carbon.

In the current study, a novel  $sp^3$ -hybridized crystalline carbon allotrope with C-centered orthorhombic structure is reported. There are 8 atoms per primitive cell (Cco-C<sub>8</sub>), which has (2, 2) CNTs interlinked through 4- and 6-member rings predicted by using a recently developed particle-swarm optimization algorithm on structural search [18–21]. In fact, Cco-C<sub>8</sub> can be obtained from direct compression on periodic (2, 2) and (4, 4) CNTs. The simulated XRD pattern, crystal density, bulk modulus, and hardness of Cco-C<sub>8</sub> are in satisfactory agreement with experimental observations on quenched products from compressed bundled CNTs [14]. Cco-C<sub>8</sub> is energetically

more favorable than *M* carbon, bct- $C_4$ , *W* carbon, and chiral  $C_6$  over the wide range of pressures.

The structural search for carbon allotropes with simulation cell sizes up to 28 atoms in the pressure range 0–100 GPa was performed with particle-swarm optimization methodology as implemented in the Crystal Structure Analysis by Particle Swarm Optimization (CALYPSO) code [18–21]. The CALYPSO method was designed to predict stable or metastable crystal structures requiring only chemical compositions of a given compound at specified external conditions (e.g., pressure), unbiased by any known structural information. The CALYPSO method has been very successful in predicting several structures which were subsequently confirmed by independent experiments [18–21]. Underlying structural relaxations were performed by using density functional theory within the local density approximation (LDA) as implemented in the Vienna Ab Initio Simulation Package code [22]. The all-electron projector augmented wave method [23] was adopted with  $2s^22p^2$  treated as valence electrons. A plane-wave basis set with an energy cutoff of 1000 eV was used, which gave well-converged total energies of  $\sim 1$  meV/atom. The phonon frequencies for Cco- $C_8$  were calculated by using the direct supercell method, which uses the forces obtained by the Hellmann-Feynman theorem.

Structural simulations through the CALYPSO code readily yielded the experimentally known structures of graphite and diamond and earlier theoretically proposed bct- $C_4$  [4,5], chiral  $C_6$  [24], *M* carbon [3], and *W* carbon [6]. An unexpected novel C-centered orthorhombic  $Cmmm$  structure (16 atoms/unit cell, Fig. 1) was found in the simulation of 8 atoms/cell, energetically more favorable than *M* carbon, *W* carbon, bct- $C_4$ , chiral  $C_6$ , and 3D-(6,0) carbon in the wide pressure range studied (Fig. 2). At zero pressure, the optimized lattice parameters of Cco- $C_8$  are  $a = 8.674$  Å,  $b = 4.209$  Å, and  $c = 2.487$  Å with carbon atoms occupying  $8q$  ( $-1/6, -0.815, -1/2$ ) and  $8p$  ( $-0.089, -0.315, 0$ ) Wyckoff positions. Cco- $C_8$  shares structural similarity with armchair (2, 2) CNTs, bct- $C_4$ , and graphite and can be viewed as 3D polymers of (2, 2) CNTs interconnected through 4- and 6-member rings [Fig. 1(a)]. Although bct- $C_4$  also consists of (2, 2) CNTs, its interconnection is solely realized by 4-member rings [Fig. 1(c)]. The top view along the  $b$  axis [Fig. 1(b)] reveals the structural similarity with graphite, where AA-stacked reconstruction of the graphene layer is seen by the formation of wrinkled layers as a result of interlayer bonding.

The thermodynamic stability of Cco- $C_8$  was examined by a direct enthalpy comparison with known experimental and theoretical carbon allotropes (Fig. 2). Except for the experimental graphite, lonsdaleite, and diamond structures, Cco- $C_8$  is energetically more favorable than all earlier theoretical structures and surpasses graphite above 9.3 GPa. The appearance of diamondlike 6-member rings in Cco- $C_8$  might be the key for lowering the energy. In

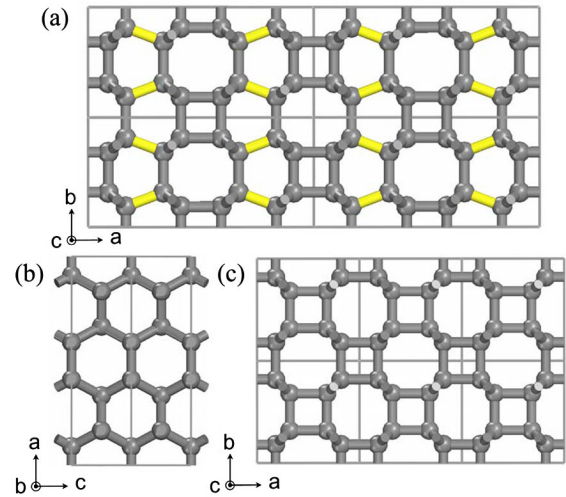


FIG. 1 (color online). Top views of crystal structures of Cco- $C_8$  (a),(b) and bct- $C_4$  (c). (a) and (c) are views along the  $c$  axis, whereas (b) is a view along the  $b$  axis. The yellow bonds indicate the six atom rings of Cco- $C_8$ .

other polymorphs, the presence of 4 + 8 rings in bct- $C_4$  and 5 + 7 rings in *M* carbon and *W* carbon is apparent. The dynamic stability of Cco- $C_8$  at zero pressure was verified by calculating its full phonon dispersion spectra. No imaginary frequencies were observed throughout the whole Brillouin zone [25]. The calculated electronic band structure at zero pressure [25] gives an insulating feature to Cco- $C_8$  with an indirect band gap of 3.12 eV, which is between 2.56 eV for bct- $C_4$  [5] and 3.6 eV for *M* carbon [3]. Since density functional calculations usually underestimate the band gaps, larger values from real experiments are expected.

Cco- $C_8$  has a high bulk modulus of 444.1 GPa (Table I), high crystal density (3.51 g/cm<sup>3</sup>), and high Vickers hardness of 95.1 GPa, as derived from our microscopic hardness model [27–29]. Although these excellent mechanical properties are slightly inferior to those of diamond, they are better than other proposed carbon polymorphs

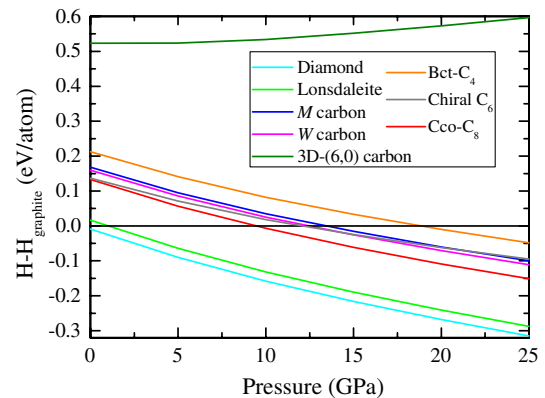


FIG. 2 (color online). Enthalpy differences of various carbon allotropes relative to graphite.

TABLE I. Calculated equilibrium volume  $V_0$  ( $\text{\AA}^3/\text{atom}$ ), band gap  $E_g$  (eV), bulk modulus  $B_0$  (GPa), and Vickers hardness  $H_v$  (GPa) of diamond,  $M$  carbon,  $W$  carbon, bct- $C_4$ , chiral  $C_6$ , and Cco- $C_8$  at zero pressure. Other theoretical data [3,5,6,24] and experimental data [26] are also listed for comparison.

| Structure    | Method                                  | $V_0$ | $E_g$ | $B_0$ | $H_v$ |
|--------------|---|-------|-------|-------|-------|
| Diamond      | This work                               | 5.52  | 4.19  | 466.8 | 97.5  |
|              | LDA [6]                                 | 5.52  | 4.20  | 466.3 |       |
|              | LDA [3]                                 | 5.52  |       | 468.5 |       |
|              | Expt. [26]                              | 5.67  | 5.47  | 446   |       |
| $M$ carbon   | This work                               | 5.78  | 3.55  | 432.4 | 93.5  |
|              | LDA [3]                                 | 5.78  | 3.6   | 431.2 |       |
|              | LDA [5]                                 | 5.77  |       | 428.9 |       |
| $W$ carbon   | This work                               | 5.77  | 4.35  | 431.7 | 93.8  |
|              | LDA [6]                                 | 5.76  | 4.39  | 444.5 |       |
| bct- $C_4$   | This work                               | 5.83  | 2.62  | 431.2 | 92.9  |
|              | LDA [5]                                 | 5.82  | 2.56  | 428.7 |       |
|              | LDA [6]                                 | 5.83  | 2.58  | 433.7 |       |
| Chiral $C_6$ | This work                               | 6.03  | 3.72  | 416.2 | 90.8  |
|              | Generalized gradient approximation [24] | 6.20  | 4.12  | 390   |       |
| Cco- $C_8$   | This work                               | 5.68  | 3.12  | 444.1 | 95.1  |

(Table I). These mechanical properties are in accordance with experimental observations on the undetermined carbon phase recovered from cold-compressed CNTs, which has a density of  $3.6 \pm 0.2 \text{ g/cm}^3$  and a bulk modulus of 447 GPa [14]. The simulated hardness of 95.1 GPa can naturally explain the presence of indentation marks along with radial cracks on the defect-free single crystal diamond anvil [14].

To enhance the validity of the Cco- $C_8$  structure, we carried out a direct comparison of its XRD pattern with the experimental data [14], as depicted in Fig. 3. Earlier proposed 3D-(6, 0) carbon is also presented for comparison. The simulated angle-dispersive XRD results were converted into energy-dispersive data for better comparison with the experiments [30]. Although the experimental XRD peaks are of low resolution and generally weak, four main peaks of Cco- $C_8$  at  $d$  spacings of 2.158, 2.079, 1.507, and 1.250  $\text{\AA}$  give satisfactory comparisons in positions and intensities with the experimental  $d$  spacings of 2.155, 2.053, 1.495, and 1.248  $\text{\AA}$  [14]. In contrast, 3D-(6, 0) carbon is clearly absent in the XRD peak at a  $d$  spacing of 2.155  $\text{\AA}$ , whereas the strong peak ( $d$  spacing = 1.848  $\text{\AA}$ ) appears at  $E = 35 \text{ keV}$ , which is inconsistent with the experimental result. Comparison of the XRD of Cco- $C_8$  with that of the superhard carbon derived from cold-compressed graphite was attempted. Significant deviation with the experimental XRD data was found, ruling out the possibility of Cco- $C_8$  as the candidate for the structure of the experimentally observed superhard carbon [25].

Geometrically, Cco- $C_8$  is intimately correlated with the  $(n, n)$  CNTs because it is made up of (2, 2) CNTs

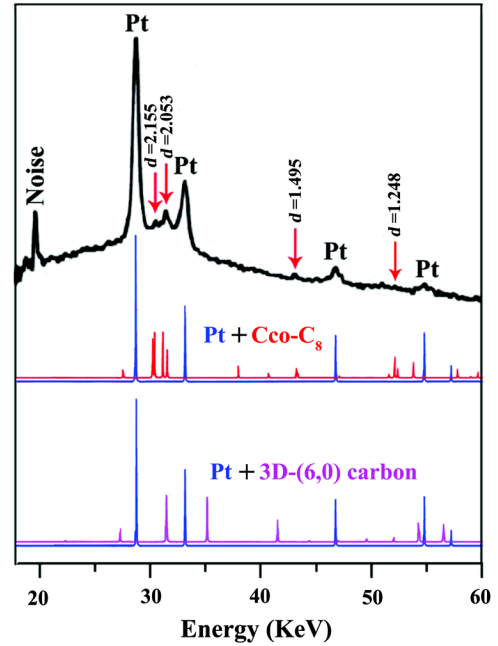


FIG. 3 (color online). Simulated XRD patterns of Cco- $C_8$  and 3D-(6, 0) carbon at ambient pressure, compared with experimental data [14]. Pt, blue lines; Cco- $C_8$ , red lines; 3D-(6, 0) carbon, violet lines; experimental XRD, black lines. The red arrows point to four main peaks of experimental product.

interconnected by  $sp^3$  bonds. Transition path simulation reveals the easy formation of Cco- $C_8$  through isotropic compression of the (2, 2) CNT bundle. The transition accompanies the shortened nearest intertube distances from 3.35  $\text{\AA}$  at 0 GPa to 1.54  $\text{\AA}$  at 5 GPa, which is a critical pressure for the formation of Cco- $C_8$ . Further simulations under nonhydrostatic pressure show that Cco- $C_8$  can actually be formed from the compression of other  $(n, n)$  CNTs, where  $n = 4, 6, \dots$ , with larger tube diameters. The mechanism by which the (4, 4) CNT bundle transforms into Cco- $C_8$  upon compression is simulated and presented in Fig. 4. A nonhydrostatic pressure is required to drive the transition. The (4, 4) CNT bundle [Fig. 4(a)] is first polymerized under pressure to form a 3D-(4, 4) nanotube polymer [31] [Fig. 4(b)] along the  $a$  and  $b$  coordinate axes by (2 + 2) cycloaddition. This is similar to the formation process of known 3D  $C_{60}$  polymers [7–10]. The polymer is further distorted and becomes flatter with continued compressions [Figs. 4(c) and 4(d)], eventually leading to the formation of the Cco- $C_8$  structure [Fig. 4(e)]. Other larger  $(n, n)$  CNTs can also be pressurized into Cco- $C_8$  structures by using a mechanism similar to that described above. Energetically, (2, 2) CNT in isolation has a higher energy than other typical nanotubes [e.g., 0.70 eV/atom higher in energy than (6, 0) CNT] [31]. Even so, (2, 2) CNTs can still be experimentally grown inside a multiwalled CNT [32]. Energies of  $(n, n)$  CNTs decrease with increasing tube diameters. As a consequence, (4, 4) CNT becomes energetically more favorable than (6, 0) CNTs [31].

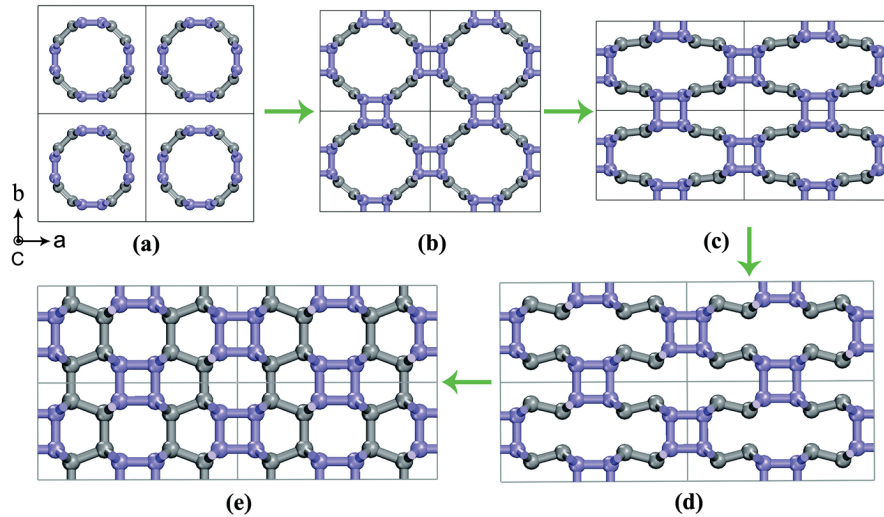


FIG. 4 (color online). Mechanism of transformation of (4,4) CNT bundles into Cco-C<sub>8</sub> structures under nonhydrostatic pressure. (a) (4,4) CNT bundle; (b) 3D-(4,4) nanotube polymer [31]; (c),(d) distorted 3D-(4,4) nanotube polymers; and (e) Cco-C<sub>8</sub>. The applied pressure is 69 GPa along the *a* axis and 70 GPa along the *b* and *c* axes, respectively.

Carbon has a rich chemistry, which allows the formation of a large number of carbon allotropes with various C-C covalent bonds. The peculiarity is responsible for the existence of many metastable carbon phases. It is not surprising to see many nearly degenerated energetic carbon phases in certain pressure ranges (e.g., for *sp*<sup>3</sup> crystals, Cco-C<sub>8</sub>, *M* carbon, *W* carbon, and chiral C<sub>6</sub> have similar energies at elevated pressures of up to 25 GPa, as shown in Fig. 2). As a consequence, the energy criteria cannot be solely relied on for a precise theoretical determination of certain carbon phases. One might not guess that high-energy CNTs can be actually synthesized if without the experimental evidence. These arguments are generally true in view of the complexity of carbon. However, it does not go against the current proposal on the validity of the Cco-C<sub>8</sub> phase, having a preferable energy in comparison with other theoretical structures. The Cco-C<sub>8</sub> structural model is also supported by other evidence, including the excellent agreement between theory and experiment on the density and bulk modulus. The experimental density ( $3.6 \pm 0.2$  g/cm<sup>3</sup>) is an average density, and it is possible that there is a non-negligible presence of defects and amorphous carbon on the grain boundary. Moreover, the experimental density is determined by an uncertain *P*-62c structure. Although structural deviation might lead to modification of density, large density changes are not expected because of the similar *sp*<sup>3</sup> bonding dominance.

In summary, a recently developed CALYPSO technique for structural search was employed, and a novel superhard carbon allotrope Cco-C<sub>8</sub> was successfully uncovered. This new carbon form is energetically more stable than earlier theoretical structures and can account for experimental observations on the XRD, density, and hardness of a quenched product recovered from cold-compressed CNT bundles. The current study suggests a route for the

synthesis of novel 3D crystals by directly compressing CNT bundles in a manner similar to experimentally obtained 3D C<sub>60</sub> polymers. More novel synthesized carbon materials with unique physical properties are expected by pressure-induced polymerization of various CNTs.

This work was supported by NSFC (Grants No. 50821001, No. 51025103, No. 91022029, and No. 11174152), NBRPC (Grant No. 2011CB808205), and the Science Foundation of Yanshan University for the Excellent Ph.D. Students (Grant No. YSUSF201101).

\*fhcl@ysu.edu.cn

- [1] E.D. Miller, D.C. Nesting, and J.V. Badding, *Chem. Mater.* **9**, 18 (1997).
- [2] W.L. Mao, H.K. Mao, P.J. Eng, T.P. Trainor, M. Newville, C.C. Kao, D.L. Heinz, J.F. Shu, Y. Meng, and R.J. Hemley, *Science* **302**, 425 (2003).
- [3] Q. Li, Y.M. Ma, A.R. Oganov, H.B. Wang, H. Wang, Y. Xu, T. Cui, H.K. Mao, and G.T. Zou, *Phys. Rev. Lett.* **102**, 175506 (2009).
- [4] X.-F. Zhou, G.-R. Qian, X. Dong, L.X. Zhang, Y.J. Tian, and H.T. Wang, *Phys. Rev. B* **82**, 134126 (2010).
- [5] K. Umemoto, R.M. Wentzcovitch, S. Saito, and T. Miyake, *Phys. Rev. Lett.* **104**, 125504 (2010).
- [6] J.-T. Wang, C.F. Chen, and Y. Kawazoe, *Phys. Rev. Lett.* **106**, 075501 (2011).
- [7] L. Marques, J.-L. Hodeau, M. Nunez-Regueiro, and M. Perroux, *Phys. Rev. B* **54**, R12 633 (1996).
- [8] V.D. Blank, S.G. Buga, G.A. Dubitsky, N.R. Serebryanaya, M. Yu. Popov, and B. Sundqvist, *Carbon* **36**, 319 (1998).
- [9] S.J. Yamanaka, A. Kubo, K. Inumaru, K.J. Komaguchi, N.S. Kini, T. Inoue, and T. Irifune, *Phys. Rev. Lett.* **96**, 076602 (2006).

- [10] E. Y. Tonkov and E. G. Ponyatovsky, *Phase Transformations of Elements under High Pressure* (CRC, Boca Raton, FL, 2005).
- [11] M. Popov, M. Kyotani, R. J. Nemanich, and Y. Koga, *Phys. Rev. B* **65**, 033408 (2002).
- [12] M. Popov, M. Kyotani, and Y. Koga, *Diam. Relat. Mater.* **12**, 833 (2003).
- [13] V. N. Khabashesku, Z. N. Gu, B. Brinson, J. L. Zimmerman, J. L. Margrave, V. A. Davydov, L. S. Kashevarova, and A. V. Rakhmanina, *J. Phys. Chem. B* **106**, 11 155 (2002).
- [14] Z. W. Wang, Y. S. Zhao, K. Tait, X. Z. Liao, D. Schiferl, C. S. Zha, R. T. Downs, J. Qian, Y. T. Zhu, and T. D. Shen, *Proc. Natl. Acad. Sci. U.S.A.* **101**, 13 699 (2004).
- [15] R. S. Kumar, M. G. Pravica, A. L. Cornelius, M. F. Nicol, M. Y. Hu, and P. C. Chow, *Diam. Relat. Mater.* **16**, 1250 (2007).
- [16] J. Tang, L.-C. Qin, T. Sasaki, M. Yudasaka, A. Matsushita, and S. Iijima, *Phys. Rev. Lett.* **85**, 1887 (2000).
- [17] M. J. Bucknum and E. A. Castro, *J. Chem. Theory Comput.* **2**, 775 (2006).
- [18] Y. C. Wang, J. Lv, L. Zhu, and Y. M. Ma, *Phys. Rev. B* **82**, 094116 (2010).
- [19] P. F. Li, G. Y. Gao, Y. C. Wang, and Y. M. Ma, *J. Phys. Chem. C* **114**, 21745 (2010).
- [20] J. Lv, Y. C. Wang, L. Zhu, and Y. M. Ma, *Phys. Rev. Lett.* **106**, 015503 (2011).
- [21] L. Zhu, H. Wang, Y. C. Wang, J. Lv, Y. M. Ma, Q. L. Cui, Y. M. Ma, and G. T. Zou, *Phys. Rev. Lett.* **106**, 145501 (2011).
- [22] G. Kresse and J. Furthmuller, *Phys. Rev. B* **54**, 11 169 (1996).
- [23] P. E. Blochl, *Phys. Rev. B* **50**, 17 953 (1994).
- [24] Chris J. Pickard and R. J. Needs, *Phys. Rev. B* **81**, 014106 (2010).
- [25] See Supplemental Material at <http://link.aps.org/supplemental/10.1103/PhysRevLett.107.215502> for additional electronic and dynamical properties.
- [26] F. Occelli, P. Loubeyre, and R. Letoullec, *Nature Mater.* **2**, 151 (2003).
- [27] F. M. Gao, J. L. He, E. D. Wu, S. M. Liu, D. L. Yu, D. C. Li, S. Y. Zhang, and Y. J. Tian, *Phys. Rev. Lett.* **91**, 015502 (2003).
- [28] J. L. He, E. D. Wu, H. T. Wang, R. P. Liu, and Y. J. Tian, *Phys. Rev. Lett.* **94**, 015504 (2005).
- [29] X. J. Guo, L. Li, Z. Y. Liu, D. L. Yu, J. L. He, R. P. Liu, B. Xu, Y. J. Tian, and H. T. Wang, *J. Appl. Phys.* **104**, 023503 (2008).
- [30] M. Croft, V. Shukla, E. K. Akdoğan, N. Jisrawi, Z. Zhong, R. Sadangi, A. Ignatov, L. Balarinni, K. Horvath, and T. Tsakalakos, *J. Appl. Phys.* **105**, 093505 (2009).
- [31] Z. S. Zhao, B. Xu, L.-M. Wang, X.-F. Zhou, J. L. He, Z. Y. Liu, H.-T. Wang, and Y. J. Tian, *ACS Nano* **5**, 7226 (2011).
- [32] X. Zhao, Y. Liu, S. Inoue, T. Suzuki, R. O. Jones, and Y. Ando, *Phys. Rev. Lett.* **92**, 125502 (2004).